Uncertainty Assessment of Local SAR Mapping from Radiofrequency Induced Heating of a Standardized 10.0 cm Long Titanium Rod in the ASTM Phantom at 64 and 128 MHz

Krzysztof Wawrzyn, Jack Hendriks, William B. Handler, Blaine A. Chronik
The xMR Labs, Department of Physics and Astronomy, Western University, London ON, Canada

PURPOSE: The purpose of this study was to quantify the measurement uncertainty in local specific absorption rate (LSAR) inside a standard gel-filled ASTM phantom. LSAR was repeatedly measured over various spatial distributions in and near the standard implant testing location within the ASTM phantom, for exposure to circularly polarized RF fields at both 64 and 128 MHz.

INTRODUCTION: The *in vitro* assessment of LSAR is described in the technical specifications standard of ASTM International F2182-11a [1], by direct measure of RF-induced heating of an elongated conductive 10.0 cm long titanium (Ti) rod within a standardized phantom. A frequency dependent scaling factor for the rod normalizes the measured temperature rise to a LSAR value that would be present in the rods absence [1]. The SAR distribution depends on the employed RF coil design and phantom shape and size. It is necessary to know the LSAR distribution accurately prior to medical implant device testing in order to achieve a meaningful assessment. A key measurement parameter is the uncertainty associated with the physical measurement process. In this study, we exploit the RF-related heating on a 10 cm long Ti rod to measure the LSAR deposited in and around the implant testing location by scaling the measured temperature rise at both 64 and 128 MHz.

METHODS: All measurements were performed on two different RF bench top exposure systems, commercially available as Medical Implant Test Systems, or MITS 1.5 (64 MHz) and MITS 3.0 (128 MHz) [2]. The MITS 1.5 & 3.0 sequence parameters (Software v1.12.10, [2]) were: RF duration = 360 s, pulse type = sinc2π, duty cycle = 40 %, pulse repetition rate = 1 kHz, polarization = circular 270 ° & 90 °, frequency = 63.34 & 127.60 MHz, input power = 59.0 & 60.2 dBm, whole-body SAR = 2.97 ± 0.04 & 3.01 ± 0.18 W/kg, and $B_{1,rms}$ = 2.86 & 4.40 µT in air at the coils' geometric isocenter. **Figure 1** shows a 3-D illustration of the measurement setup. An ASTM specific human torso acrylic phantom (42×65×16.5 cm) was filled with a gelled saline made of Hydroxyethyl cellulose (HEC), formulated to match the electrical conductivity (0.47 S/m ± 10 %) and worst case thermal convection properties (i.e. without perfusion) of human tissue, to a gel height of 9.0 cm. The geometric center of the phantom gel (height of 4.5 cm) was aligned with the geometric center of the MITS. The 10.0 cm long rod was machined from 1/8-inch diameter Grade 5 Ti, with two 1.0 mm diameter holes drilled through and placed 1.0 mm from each end of the rod.

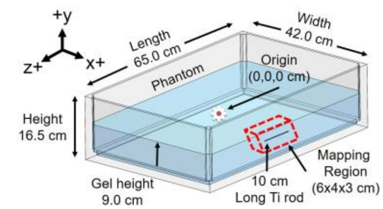

Figure 1: 3-D illustration of phantom container with 10 cm Ti rod at the center of the mapping region for a LSAR measurement at 128 MHz.

A 0.60 mm diameter T1C fiber optic temperature sensor [3] (resolution = 0.1 °C, accuracy = 0.2 °C) was placed in the symmetrically opposed holes to monitor temperature with a calibrated Omniflex signal conditioner [3]. Temperature data were taken at points submerged in the gel parallel to the long-sided wall at different spatial increments (1.0 to 2.0 cm) centered on the typical implant testing location, originating 33 mm from the x-axis wall and 52 mm from the phantom floor (y-axis). The measured temperature change from the 10.0 cm rod was normalized by a LSAR scalar factors of 1.30 and 1.45 °C/W/kg for 64 and 128 MHz, respectively [1]. The center test location LSAR value, V_c, was compared to the surrounding LSAR values, V_s, by using percent difference: $|V_s - V_c|/(\frac{\sum V}{2}) \times 100$.

RESULTS AND DISCUSSION: A representative 3-D scatter plot map of LSAR values with corresponding bar graphs is shown in **Figure 2**. **Table 1** shows a summary of peak LSAR percent differences. Percent differences have also been estimated by modifying the position change to 1.0 cm. At 128 MHz, the highest percent differences were along the y- and diagonal-directions, with up to 27.35 % and 17.62 % difference for a 1.0 cm position change, respectively. The LSAR difference along y-axis was 9× and 32× greater compared to x- and z-axis changes at 128 MHz. At 64 MHz, the percent differences for 1.0 cm position change along x, y and diagonally were in the range of 8.24–10.39 %. A low percent difference (< 0.85 %) along z-axis for both systems is consistent with the expected uniform LSAR distribution along z-axis. Further mapping can be performed with different E-field/SAR probes, such as those commercially available [4] and in house [5], as well as simulations to verify and validate the findings.

Table 1: Summary of highest percent differences for LSAR values.

MITS	dz (2.0cm)	dx (1.35cm)	dy (1.0cm)	Diag. (2.61cm)	dz' (1.0cm)	dx' (1.0cm)	dy' (1.0cm)	Diag.' (1.0cm)
3.0	1.71%	4.03%	27.35%	46.01%	0.85%	3.00%	27.35%	17.62%
1.5	1.63%	11.13%	7.69%	27.13%	0.82%	8.24%	7.69%	10.39%

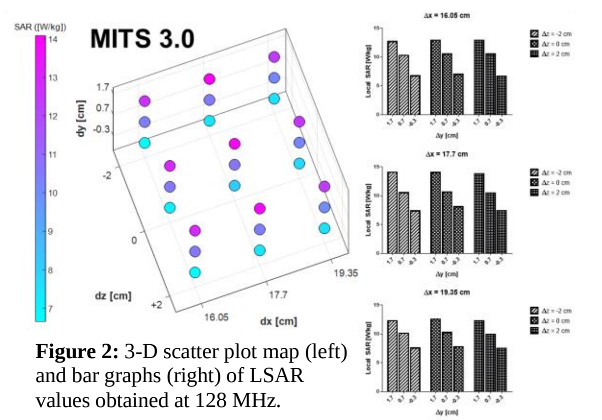

Figure 2: 3-D scatter plot map (left) and bar graphs (right) of LSAR values obtained at 128 MHz.

CONCLUSION: This work was conducted to provide additional and direct experimental quantification of the actual measurement uncertainty associated with SAR probe positioning. We have quantified the extent to which the LSAR in a standardized phantom surrounding a device implant assessment location during RF testing will change with device placement. These experimental maps can be used to define the contribution that device placement makes to total measurement uncertainty in device heating measurements.

ACKNOWLEDGEMENTS: The authors would like to thank Ryan Chaddock, Brian Dalrymple, and Frank Van Sas for technical support. This work was funded by NSERC Industrial Research Chairs Program, Ontario Research Fund Research Excellence Program, and Canadian Foundation for Innovation.

REFERENCES: [1] ASTM F2182: Test Method for Measurement of Radio Frequency Induced Heating On or Near Passive Implants During Magnetic Resonance Imaging. Pennsylvania, USA: ASTM International, 2013. [2] (ZMT, Zurich, Switzerland). [3] (Neoptix, Québec, Canada). [4] (Speag, Zurich, Switzerland). [5] A. Attaran, et al. IEEE Trans. Antennas Propag., 2017.